Influence of tissue mechanical strength during UV and IR laser ablation in vitro

Jansen, E. Duco, van Leeuwen, Ton, Verdaasdonck, Rudolf, Le, Tuong, Motamedi, Massoud, et al.

E. Duco Jansen, Ton G. J. M. van Leeuwen, Rudolf M. Verdaasdonck, Tuong H. Le, Massoud Motamedi, Ashley J. Welch, Cornelius Borst M.D., "Influence of tissue mechanical strength during UV and IR laser ablation in vitro," Proc. SPIE 1882, Laser-Tissue Interaction IV, (7 July 1993); doi: 10.1117/12.147654

Event: OE/LASE'93: Optics, Electro-Optics, and Laser Applications in Scienceand Engineering, 1993, Los Angeles, CA, United States

Influence of Tissue Mechanical Strength During UV and IR Laser Ablation *in Vitro*

E. Duco Jansen[1], Ton G. van Leeuwen[2], Rudolf M. Verdaasdonk[3], Tuong H. Le[1], Massoud Motamedi[4], A.J. Welch[1] and Cornelius Borst [2]

1 Biomedical Engineering Program, University of Texas, Austin TX 78712
2 Experimental Cardiology Laboratory, University Hospital Utrecht, and Interuniversity Cardiology Institute of The Netherlands
3 Medical Laser Center, University Hospital Utrecht, The Netherlands
4 Biomedical Laser Center, University of Texas Medical Branch, Galveston TX

ABSTRACT

It is has been established that the infrared (Ho:YAG at 2.09 μm) ablation process involves direct heating of tissue water followed by subsurface pressure build up that ultimately leads to a violent explosion. Recently, we presented evidence that the same mechanism plays a role in ultraviolet (XeCl at 308 nm) ablation. It is expected that this process is dependent upon the mechanical strength of the irradiated tissue. A qualitative study was done to demonstrate the effect of the tissue mechanical properties on the pulsed laser ablation process and resulting mechanical damage to tissue.

A Ho:YAG laser (SEO 1-2-3 with λ = 2.09 μm, repetition rate = 2 Hz, pulsewidth = 250 μs FWHM) and a XeCl excimer laser (Technolas MAX-10, with λ = 308 nm, repetition rate = 2 Hz, pulsewidth = 115 ns) were used to study the effects of tissue strength during ablation. The Ho:YAG and XeCl laser beams were coupled into 600 and 950 μm diameter fibers respectively, and irradiances were 1.06 J/mm^2 and 47 mJ/mm^2, respectively. Beef myocardium, beef liver, pig aorta, pig cornea, cartilage (pig ear), and bone were irradiated *in vitro* under saline; also saline was irradiated as a control. The ablation process was documented with a fast flash photography setup and histology was performed on all tissue samples.

During holmium ablation, the stronger tissue (aorta) contained the vapor bubble subsurface, where as the weak and/or looser tissues (liver, myocardium) did not confine the bubble. In the latter tissues the bubble appeared as hemisphere on top of the tissue. In cartilage, no bubble or tissue elevation was observed during ablation. In case of bone ablation, the formation of a steam plume on top of the bone was seen. During excimer laser ablation of these tissues under saline, similar vapor bubbles were observed.

Histology showed that in the mechanically 'weak' tissues a larger crater was formed with greater mechanical damage to the adjacent tissue. There was a correlation between the maximum bubble size and the extent of mechanical damage to the tissue. In conclusion, during infrared and ultraviolet laser ablation, the mechanical properties of the ablated tissue influence the ablation process.

1. INTRODUCTION

The two main laser groups that are currently being used for tissue ablation with relative little thermal damage to the adjacent tissue are the ultraviolet (UV) excimer lasers (i.e. XeCl at 308 nm) and the mid infrared (IR) lasers (i.e. Ho:YAG at 2.09 μm)[1]. In the past few years research and prototype systems for ablation have focused on angioplasty[2,3] and opthalmology.[4,5] However, more recently the use of pulsed lasers for tissue ablation is also being explored for other disciplines such as dentistry[6], urology[7], orthopedic surgery[8], and otolaryngology[9]. It was noted that the pulsed excimer laser as well as the pulsed holmium laser caused significant mechanical damage to the surrounding tissue during ablation.[10] Models for pulsed laser ablation typically consider only the optical and thermal properties of the irradiated material. Using a pulsed laser, the deposition of energy and heating of the tissue are rapid. Because there may be insufficient time for the expansion of heated (tissue)water, there can be a significant pressure increase followed by a violent explosion. This phenomena of superheating water was first described by researchers in materials science.[11,12] However, it was not until very recently that the actual explosive vaporization of tissue water was documented.[13] It is now well established that the IR ablation process involves direct heating of tissue water followed by subsurface pressure build up that ultimately leads to a violent explosion.

Given the awareness that pulsed laser ablation involves large pressure increases within tissue and the explosive nature of the process, it is expected that the process is dependent upon the mechanical strength of the irradiated tissue. There are few published studies that describe a comparison of different tissues with different mechanical properties but similar optical and thermal properties. Walsh *et al.*[14] described the effect of mechanical properties for pulsed CO_2 laser ablation and concluded that "mechanical strength of tissue can affect mass removal by pulsed laser ablation by as much as a factor of

0-8194-1109-4/93/$6.00

seven." Thus mechanical properties are very important in the modeling, interpretation and precise control of pulsed laser ablation.

In this paper we will, in a *qualitative* way, describe the effect of the mechanical strength of tissue on the ablation process with pulsed UV and IR lasers, and try to relate the differences during the ablation process, documented using fast flash photography, to mechanical damage around the ablation crater as observed with standard histological techniques.

2. MATERIALS AND METHODS

Two different lasers were used in this study. For the IR experiments we used a pulsed Ho:YAG laser (Schwartz Electro Optics 1-2-3) with a pulselength of 250 μs (FWHM), repetition rate = 2 Hz, λ = 2.09 μm and the energy per pulse = 300 mJ/p. The laser beam was coupled into a low OH optical fiber with a core diameter of 600 μm. At the fiber tip the irradiance is 1.06 J/mm^2 and is assumed to be uniform.

For the UV experiments we used a XeCl excimer laser (Technolas, Max 10) with a pulselength of 115 ns, repetition rate = 2 Hz, λ = 308 nm and the energy per pulse = 30 mJ/p. The laser was coupled into a fiber with a core diameter of 950 μm. At the fiber tip the irradiance is 42 mJ/mm^2.

The ablation process was documented on videotape using fast flash photography. The pulse duration of the flash is 10 μs. The setup is shown in figure 1.

Several tissues were irradiated under saline *in vitro*: beef liver, beef myocardium, porcine aorta, porcine cornea, porcine ear (elastic cartilage), canine bone (rib) and saline as a reference. The tissues were obtained shortly after dead (within 24 hours) and stored in saline moist gauze at 4 °C until the moment of use. After irradiation all samples were fixed in a buffered formalin solution and prepared for histologic examination. In all cases the tissues were irradiated with the fiber in contact with the tissue.

The video tapes were analyzed later and for all tissues the bubble length and width were measured as a function of time elapsed since the beginning of the laser pulse. However, since the bubble length can only be measured from the top of the bubble to the tissue surface and the bubble is likely to extent into the tissue, the width of the bubble at the plane of the tissue surface was used as a marker for the bubble size.

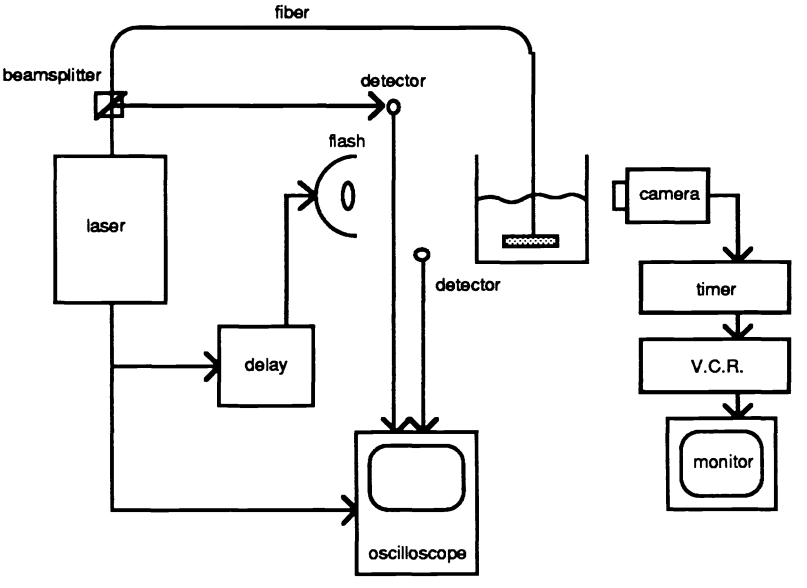

Fig. 1 . Schematic of the experimental setup

3. RESULTS

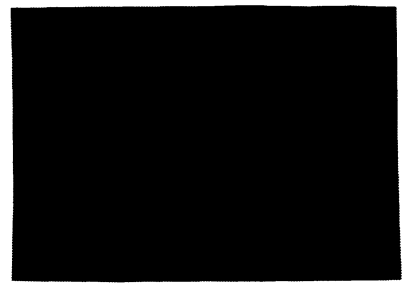

Fig. 2. Holmium:YAG laser induced bubble in saline. The fiber diameter is 600 μm. 300 mJ/p of energy was delivered, corresponding to 1.06 J/mm^2. The maximum bubble size occurs at 250 to 300 μs after the start of the laser pulse. After about 500 μs the bubble has collapsed, sometimes showing secondary bubble formation. The bubble content is assumed to be water vapor.[15]

3.1. Ho:YAG ablation

Figure 2 shows the water vapor bubble that is formed during pulsed holmium ablation of saline. In figure 3.1 - 3.6, bubble formation is shown on different tissues under saline. The same laser parameters were used as for the irradiation of saline. For every tissue, the bubble is displayed at its maximum dimensions. Just below the bubble the corresponding histological section is shown. All craters shown in histology were made with 40 pulses.

During the ablation of elastic cartilage and cornea, no appreciable bubble formation was observed and therefore these are not shown here. We can make a distinction in the behavior of the bubble on different kinds of tissue. In the very soft or structurally loose tissues (liver (fig. 3.1) and myocardium (fig. 3.2)) a large water vapor bubble is seen on top of the tissue. From one irradiation close to the edge of the tissue we know that this bubble also extends into the tissue but is not confined by the tissue. During ablation of aorta (fig. 3.3), a stronger and elastic tissue, the vapor bubble is formed and stays confined underneath the tissue surface, thus causing surface elevation. The ablation of elastic cartilage (fig. 3.5) and also cornea, both strong, elastic, collagenous tissues, with the holmium laser did not exhibit clear bubble formation. Cornea showed a heat induced whitening and structural deformation (fig. 3.6). Bone (fig. 3.4), the most dense and strongest of the tissues we used, did not show the nice round bubbles that the other tissues did. Instead we saw the ejection of an irregular steam plume of the tissue surface with small particles being dragged along by the steam cloud. This "bubble" formed sooner than the bubble on the other tissues and its lifetime was shorter. In figure 5 the maximum bubble width are shown with the time elapsed since the start of the laser pulse at which the maximum bubble width occured.

3.2. Histology of Ho:YAG laser induced craters

The appearance of the Ho:YAG induced craters was judged after microscopic evaluation on the presence and the amount of mechanical damage surrounding the ablation crater. The damage was then given a score from - to +++, where - represents a smooth crater and +++ represents a very ragged crater (fig. 6). The results are shown in figure 6. In figure 7 the maximum bubble width is plotted versus the crater appearance. There is a correlation between the maximum bubble width and the degree of mechanical damage.

3.3. Excimer ablation

Figure 4.1 - 4.5 bubble formation induced by the XeCl excimer laser is shown. The bubble, formed by a laser pulse of 30 mJ with a pulse duration of 115 ns through a 950 μm fiber is shown at 100 μs after the beginning of the laser pulse. Just below the bubble the corresponding histological section is shown. All craters shown in histology were made with 50 +/- 5 pulses. During the ablation of liver (fig. 4.1) a bubble was observed on top of the tissue. Only during the first few pulses, we sometimes observed tissue elevation. Myocardium ablation (fig. 4.2) always resulted in a vapor bubble on top of the tissue. The mechanical damage in myocardium was significant and appeared to be dependent on the directionality of the muscle fibers. In aorta we showed two different bubbles (fig 4.3 a and b). If the fiber is kept in close contact with the tissue (i.e. is allowed to penetrate into the tissue) we see significant tissue surface elevation. However, if the fiber is not kept in close contact with the tissue after a crater has started to form, we see a large water vapor bubble that appears on top of the tissue. Histologically a moderately irregular crater was left behind with dissections that extended laterally between the aorta wall layers. During the ablation of elastic cartilage (fig. 4.4) the formation of a small bubble was sometimes seen during the first few pulses. Once the fiber had penetrated into the tissue small long-lived bubbles were seen and particles together with these bubbles were ejected. Histology revealed a regular crater with several small dissections. The two large dissections at the bottom of the crater extending deeper into the tissue were no artefacts but were reproducible in 5 of 5 lesions. The ablation of porcine cornea (fig. 4.5) coincided with the release of several small long-lived bubbles. No large, fast expanding vapor bubble was observed. Histology shows a smooth and regular crater. After 50 pulses no crater formation in bone was observed. Also no bubble formation was seen with the fast flash photography.

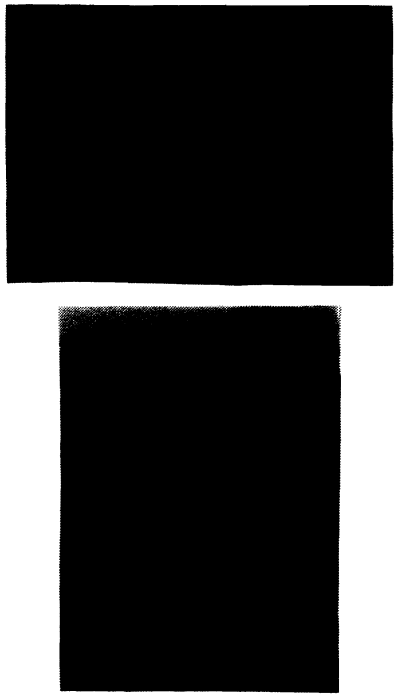

Fig. 3.1 - a) Bubble on top of beef liver during a Ho:YAG laser pulse. The maximum bubble size occured at 300 μs after the start of the laser pulse. the bubble does not stay confined in the tissue. **b)** Histological section through the crater in beef liver. The crater appearance is very ragged and significant mechanical damage to tissue adjacent to the crater is done

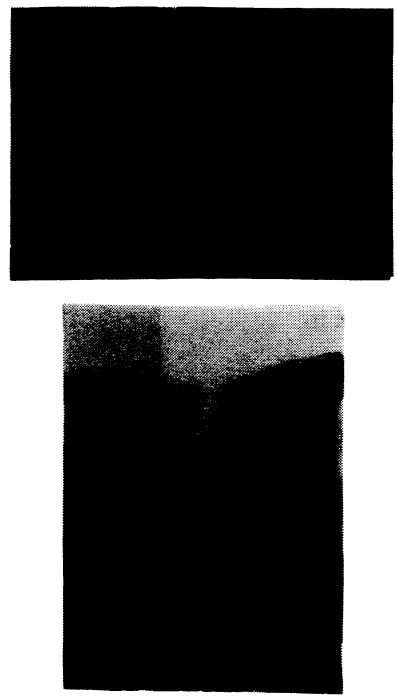

Fig. 3.2 - a) Bubble on top of beef myocardium during a Ho:YAG laser pulse. The maximum bubble size occured at 450 μs after the start of the laser pulse. The bubble does not stay confined in the tissue. **b)** Histological section through the crater in beef myocardium. The crater appearance is ragged and some mechanical damage to tissue adjacent to the crater is done

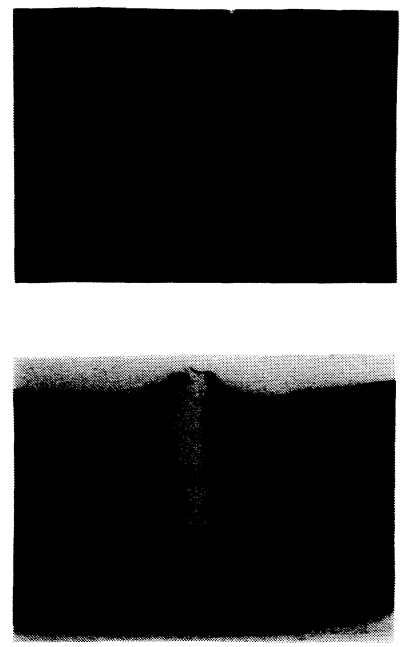

Fig. 3.3 - a) Bubble in porcine aorta during a Ho:YAG laser pulse. The maximum bubble size occured at 300 μs after the start of the laser pulse. The bubble does stay confined in the tissue and causes the tissue elevation. **b)** Histological section through the crater in porcine aorta. Dissections are seen lateral of the crater.

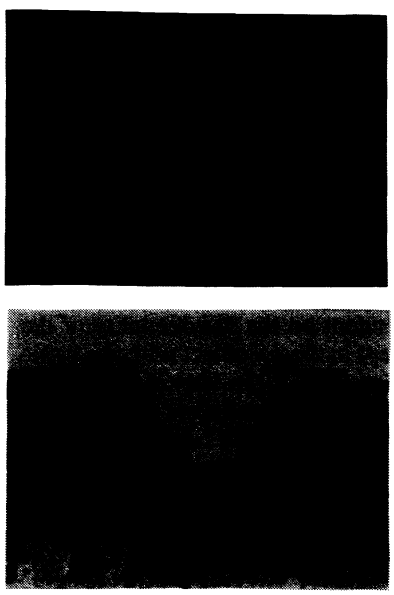

Fig. 3.4 - a) Steam plume on bone during a Ho:YAG laser pulse. The maximum plume size occured at 150 μs after the start of the laser pulse. The plume has a different appearance than the bubbles on soft tissue. **b)** Histological section through the crater in bone. The crater wall is regular and the crater is V shaped.

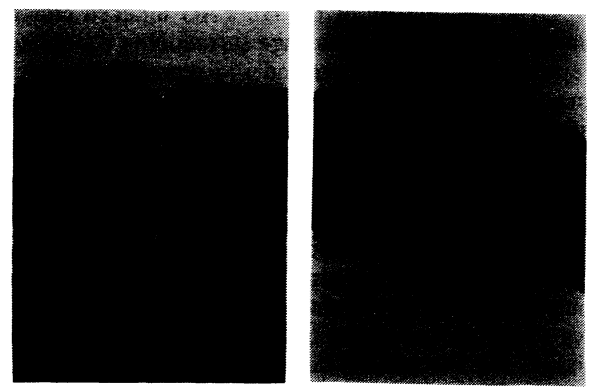

Fig. 3.5 - (left) Histological section through the crater in elastic cartilage (porcine ear). The crater wall is fairly regular. No significant bubble was observed during the laser pulse.
Fig. 3.6 - (right) Histological section through the crater in porcine cornea. The crater wall is moderately irregular. No significant bubble was observed during the laser pulse.

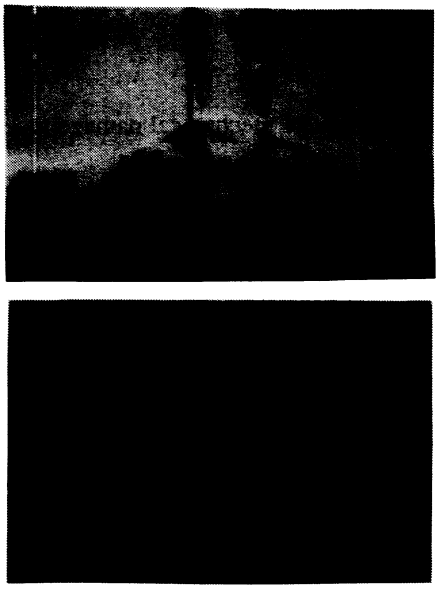

Fig. 4.1 - a) Bubble on beef liver during a excimer laser pulse. Picture was taken 100 μs after the start of the laser pulse. **b)** Histological section through the crater in beef liver. The crater appearance is ragged and significant mechanical damage to tissue adjacent to the crater is done

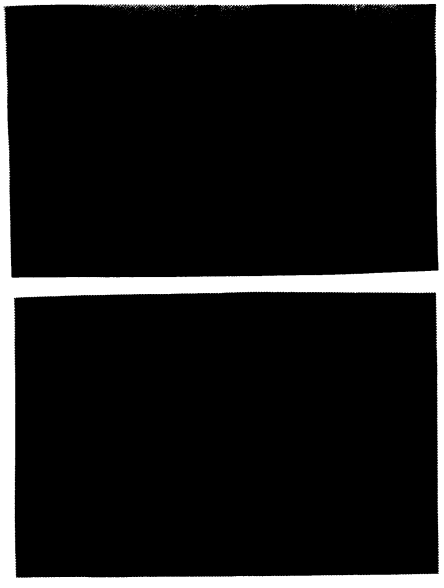

Fig. 4.4 - a) Bubble on elastic cartilage (porcine ear) during a excimer laser pulse. Picture was taken 100 μs after the start of the laser pulse. **b)** Histological section through the crater in cartilage. The crater appearance is regular with small dissections.

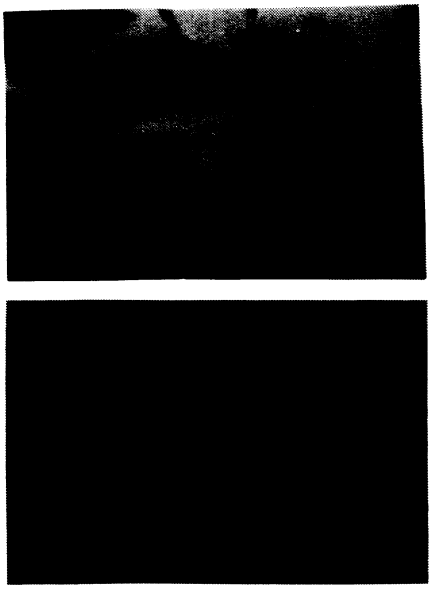

Fig. 4.2 - a) Bubble on top of beef myocardium during excimer laser pulse. Picture was taken 100 μs after the start of the laser pulse. The bubble does not stay confined in the tissue. **b)** Histological section through the crater in beef myocardium. The crater appearance is irregular and significant mechanical damage is done to tissue adjacent to the crater.

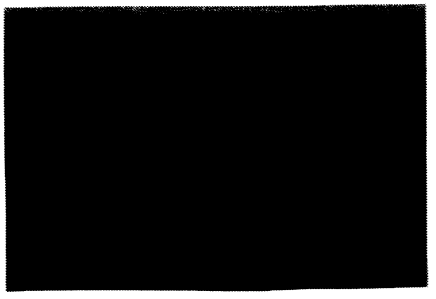

Fig. 4.5 - Histological section through the crater in porcine cornea. A very smooth crater with no mechanical damage is seen. During ablation no significant bubble formation was observed.

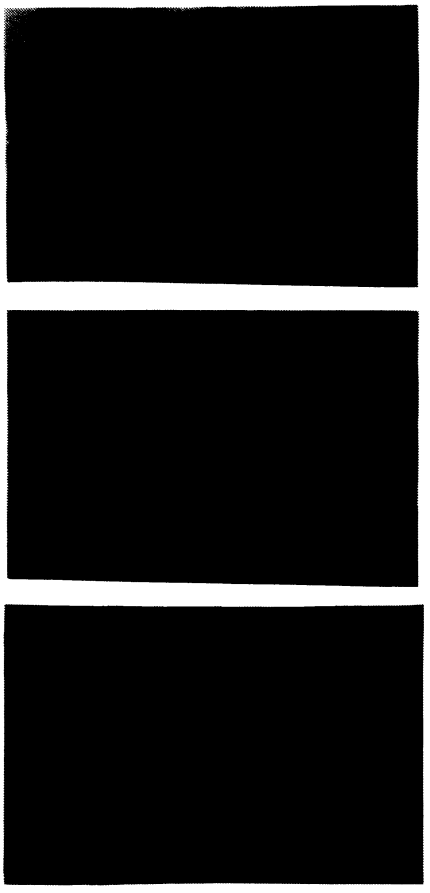

Fig. 4.3 - a) Bubble in porcine aorta during excimer laser pulse. The picture was taken 100 μs after the start of the laser pulse. The fiber is positioned inside the tissue, hence the bubble does stay confined in the tissue and causes the tissue elevation. **b)** Bubble on porcine aorta during excimer laser pulse. The picture was taken 100 μs after the start of the laser pulse. The fiber is not allowed to move into the tissue and a bubble is seen on top of the tissue. This bubble is not confined and no tissue elevation is observed. **c)** Histological section through the crater in porcine aorta. The crater is moderately irregular and dissections are seen lateral of the crater.

is shown. The amount of mechanical damage to

3.4. Histology of excimer laser induced craters

In figure 6 the histological evaluation of the excimer induced craters is shown.

Tissue	width +/- std.dev. (mm)	time (μs)
saline	2.7 +/- 0.2	250
liver	4.1 +/- 0.2	300
myocardium	2.3 +/- 0.3	400
aorta	2.1 +/- -.2	300
bone	2.3 +/- 0.2	175
cornea	-----	----
cartilage	-----	----

Fig. 5. Holmium laser induced bubble width at its maximum and the time at which the maximum size occurred. For every value given here n=5.

Tissue	Crater Appearance			
	Holmium:YAG		Excimer	
liver	very ragged	+++	ragged	++
myocardium	ragged	++	irreg.	+
aorta	dissections	+	moderately irreg	+
cornea	moderately irreg	+/-	smooth	-
cartilage	regular	+/-	small dissections	+/-
bone	regular	-	no ablation	

Fig. 6. Histological appearance of the laser induced craters. The presence and the amount of mechanical damage surrounding the ablation crater and was given a score from - to +++.

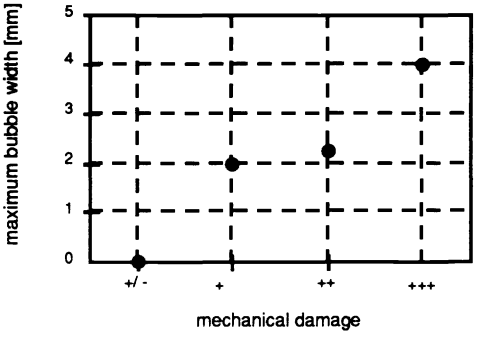

Fig. 7. The maximum bubble diameter is plotted as a function of the degree of mechanical damage. In this plot only the holmium induced bubbles and craters are considered. Also the ablation of bone is not plotted in this graph because the ablation plume appears very different from the bubbles in soft tissue ablation.

4. DISCUSSION

Holmium Ablation

We have done a qualitative study of the effects of tissue mechanical strength on ablation by pulsed Ho:YAG and excimer lasers. It was found that in soft tissues the holmium laser always causes a steam bubble to form in or on the tissue. The bubble starts to form about 50 to 100 μs after the start of the laser pulse and lasts till 500 to 800 μs after the start of the laser pulse. The mechanical strength of the tissue plays an important role.

In liver, a mechanically weak structure, a large bubble is seen and a large amount of mechanical damage is done to the tissue. In myocardium the mechanical damage is strongly dependent on the directionality of the muscle fibers. Muscle fibers are strong but are easily separated from each other. The laser induced bubble which is a high pressure vapor bubble[15,16] is able to separate the muscle fibers and thus causes a large amount of damage to the tissue. This also an explanation for the fact that a large bubble is seen on top of the tissue; the vapor can escape between the fibers and is not confined below the tissue surface. In aorta, which has a very layered structure perpendicular to the direction of laser irradiation, a similar phenomena occurs. However, in the aorta the bubble is confined by elastic lamellae in the wall, in particular the internal elastic membrane. The bubble stays confined below the tissue surface and extends laterally in between the layers of the aorta, causing the characteristic dissections lateral of the ablation crater.[10]

Cornea and cartilage are relatively strong tissues that are able to withstand the mechanical force of the holmium laser induced vapor bubble. These two tissues contain a large percentage of water so the 2.1 μm radiation is strongly absorbed. Yet, almost no bubble formation is observed during the laser ablation; the absence of bubble formation is hard to understand. Histologically this corresponds to a crater with little collateral mechanical damage. In cornea, one can also note the large zone of thermal damage induced by the multiple laser pulses. The clinical implications are that pulsed infrared laser may be able to ablate cartilage tissue such as intervertebral discs and cartilage in the knee joint with relatively little mechanical damage to surrounding tissue. In corneal ablation the pulsed infrared laser may also be used with relatively little mechanical damage. However, thermal damage would seem prohibitive.

Bone ablation appears to be quite different from the other, softer tissues. Bone has only about 10 % water content but the non-water constituents still absorb the holmium wavelength quite well. The ablation is accompanied by a large plume that is ejected from the surface of the bone. This plume also drags particles along with it. The tissue is obviously strong enough to withstand the bubble pressure and no mechanical damage is seen. It has been hypothesized that the tissue water and other absorbers, absorb the laser energy and expand, thus breaking off particles and dragging these along.[17] Our observations seem to support this hypothesis.

Excimer Ablation

Excimer laser radiation is not absorbed by water. Yet, we see bubbles that are very similar in appearance to the holmium induced water vapor bubbles. We have recently obtained evidence that the excimer bubble is indeed a water vapor bubble.[15] Hence the same mechanical properties that play a role during holmium laser ablation are expected to play a role during excimer laser ablation.

In liver we observed a large bubble on top of the tissue surface. Similar to the holmium ablation, the liver does not have the mechanical strength to withstand the fast expanding vapor bubble and significant mechanical damage is done to the tissue. Note that the laser pulse duration is only 115 ns whereas the bubble lifetime is several hundreds of μs. In myocardium the same is true as for the holmium laser; a large bubble is seen on top of the tissue and the crater appearance is very ragged. The difference with the holmium induced crater is that the tissue was oriented differently. The muscle fibers were oriented perpendicular to the direction of the laser radiation, resulting in a different pattern of mechanical damage. In aorta two bubbles are shown in figure 4.3 a and b. These two figures illustrate the importance of the fiber position relative to the tissue. If the fiber is pushed into the tissue it is tamping the crater and forcing the bubble to expand into the tissue. In non-contact the bubble is allowed to escape to the surface. It should be noted that it is still the tissue that absorbs the laser radiation unlike during holmium laser ablation where the saline in front of the fiber is absorbing the laser radiation when contact between fiber and tissue is not maintained

Ablation of cartilage with excimer laser showed a very small bubble during the first few pulses. After the first few pulses smaller long lived bubbles are formed. Histology reveals a fairly smooth crater with two dissections at the bottom of the crater extending into the tissue. The origin of these dissections, which were reproducible, is not clear.

The ablation of cornea with 308 nm excimer laser pulses resulted in a extremely smooth cut. The crater is perfectly cylindrical with a diameter equal to the fiber diameter and virtually no mechanical damage is done to the tissue. The implication is that, although no direct bond breaking is expected from photons a wavelength of 308 nm, the cut is very clean and this laser may be used for refractive surgery. Since the mechanism of ablation for this wavelength is assumed to be photo thermal and not photo chemical, the absence of mechanical and thermal damage is not easily explained.

In bone no tissue removal and/or bubble formation was observed at the fluence used (42 mJ/mm^2). In general we can conclude that the tissues that are mechanically weak suffer more mechanical damage than the stronger tissues. This

phenomena is the same as we observed during holmium:YAG ablation. In more blood rich tissues (liver, myocardium) larger bubbles are observed than in 'white' tissues. This can be explained by the hemoglobin absorption which is significant at the 308 nm wavelength.

This preliminary study is qualitative and descriptive. However, it illustrates the importance of the tissue mechanical properties for the ablation process[14]. A more quantitative assessment of tissue mechanical properties and the influence of laser irradiation on these properties is necessary in order to include mechanical tissue properties in ablation models for dosimetry calculations.

ACKNOWLEDGEMENTS

The authors want to thank Dr. Sharon Thomsen at MD Anderson Cancer Center in Houston for help with the histology. This project was sponsored by the Albert and Clemmie Caster Foundation, Office of Naval Research (under grant N00014-91-J-1564).

REFERENCES

1) Jansen E.D., Le T.H., Welch A.J., "Excimer, Ho:YAG and Q-switched Ho:YAG ablation of aorta: a comparison of temperatures and tissue damage in vitro", Appl Optics, accepted for publication:(1992).
2) Litvack F., Eigler N.L., Margolis J.R., Grundfest W.S., et al., "Percutaneous excimer laser coronary angioplasty", Am J Cardiol, 66:1027-1032 (1990).
3) Karsch K.R., Haase K.K., Mauser M., Ickrath O., et al., "Percutaneous coronary Excimer laser angioplasty in patients with coronary heart disease", Z Kardiol, 79:506-511 (1990).
4) Cotliar A.M., Schubert H.D., Mandel E.R., Trokel S.L., "Excimer laser radial keratotomy", Opthalmology, 92:206 - 208 (1985).
5) Marshall J.S., Trokel S.L., Rothery S., Schubert H.D., "An ultrastructural study of corneal incisions induced by an excimer laser at 193 nm", Opthalmology, 92:749 - 758 (1985).
6) Keller U., Hibst R., "Experimental studies of the application of the Er:YAG laser on dental hard substances: II Light microscopic and SEM investigations", Lasers Surg Med, 9:345-351 (1989).
7) Hofmann R., Hartung R., "Use of pulsed Nd:YAG laser in the ureter", Urol Clin North Am, 15:369-375 (1988).
8) Meller M., Black J., Sherk H., al. e., "Wavelength selection in laser arthroscopy", Lasers Surg Med, Suppl.3:(1991).
9) Schlenk F., Profeta G., Nelson J.S., Andrews J.A., et al., "Laser assisted fixation of ear prosthesis after stapedectomy", Lasers Surg Med, 10:444 - 447 (1990).
10) van Leeuwen T.G., van Erven L., Meertens J.H., Motamedi M., et al., "Origin of arterial wall dissections induced by pulsed excimer and mid-infrared laser ablation in the pig", J Am Coll Cardiol, 19:1610 - 1618 (1992).
11) Ready J.F., "Effects due to absorption of laser radiation", J Appl Physics, 36:462 - 468 (1965).
12) Lane R.J., Wynne J.J., Geronemus R.G., "Ultraviolet laser ablation of skin: healing studies and a thermal model", Lasers Surg Med, 6:504 - 513 (1987).
13) van Leeuwen T.G., van der Veen M.J., Verdaasdonk R.M., Borst C., "Tissue ablation by Holmium-YSGG laser pulses through saline and blood", Spie ,Bellingham, (1991).
14) Walsh J.T. Jr., Deutsch T.F., "Pulsed CO2 laser ablation of tissue: effect of mechanical properties", IEEE Trans Biomed Eng, 36:1195-1201 (1989).
15) van Leeuwen T.G., Jansen E.D., Motamedi M., Borst C., et al., "Excimer laser ablation of soft tissue: a study of the content of fast expanding and collapsing bubbles", IEEE J Quantum Electron, (submitted for publication):(1992).
16) van Leeuwen T.G., Motamedi M., Verdaasdonk R.M., Borst C., "Interaction of pulsed IR laser radiation with fluid: implication for tissue ablation", Lasers Surg Med, 3:16-16 (1991).
17) Izatt J.A., Albalgli D., Itzkan I., Feld M.S., "Pulsed laser ablation of calcified tissue: physical mechanisms and fundamental parameters", SPIE proceedings, 1202:133 -140 (1990).